$X\alpha$–SW calculations confirm,[16,22,23] that the d_{z^2} orbital becomes heavily involved in the M–M bond. The recent calculations also show that the valence-shell s and p orbitals are so high in energy that they make no significant contribution to any low-energy molecular orbitals. Apparently, then, there is no suitable empty σ-receptor orbital. The s and p_z orbitals are so high in energy that they cannot interact effectively with the stable lone-pair orbital of the potential donor atom and the d_{z^2} orbital contributes mainly to the M–M σ-bonding orbital which is filled and to the corresponding σ^* orbital which is empty but has a high energy.

To the extent that donors do form bonds in the axial position, they will tend to populate the σ^* orbital and thus tend to weaken the M–M σ bond. This in turn will weaken the π and δ bonds since the $d\pi$ and $d\delta$ overlaps, especially the latter, diminish more rapidly with distance than does the $d\sigma$–$d\sigma$ overlap. Thus, a crucial factor in opposing the formation of an axial donor bond is that not only would a certain amount of M–M σ-bond energy be lost, but this would lead to substantial losses of M–M π-bond and δ-bond energy. Even if the σ-bond situation by itself might be favorable, sizable losses in the other components of the M–M multiple bond due to their marked sensitivity to M–M distance will not energetically permit any significant relocation of the $d\sigma$ orbital from M–M bonding to M←L_{ax} bonding. Even in the very weak M←L_{ax} bonds that have been observed, we find that M–M bonds have increased in length by around 0.03–0.04 Å. Presumably this is all that can be tolerated before the $d\pi$–$d\pi$ and $d\delta$–$d\delta$ overlaps begin to fall too much.

Note Added in Proof. Since this paper was submitted, our efforts to obtain useful crystals of **1** have been unsuccessful. We are discontinuing this work; no further studies of **1** are currently planned.

Acknowledgment. We are grateful to the National Science Foundation for the support of this investigation through Grant No. MPS72-04536-A03.

Registry No. **1**, 59413-59-1; **2**·CS_2, 59389-00-3; **3**, 59389-01-4; $Mo_2(O_2CCH_3)_4$, 14221-06-8.

Supplementary Material Available: Listings of structure factor amplitudes (43 pages). Ordering information is given on any current masthead page.

References and Notes

(1) F. A. Cotton, *Chem. Soc. Rev.*, **4**, 27 (1975), and references therein.
(2) S. Trofimenko, *J. Am. Chem. Soc.*, **89**, 6288 (1967).
(3) A. B. Brignole and F. A. Cotton, *Inorg. Synth.*, **13**, 87 (1972).
(4) S. Trofimenko, *J. Am. Chem. Soc.*, **89**, 3170 (1967).
(5) R. D. Adams, D. M. Collins, and F. A. Cotton, *J. Am. Chem. Soc.*, **96**, 749 (1974).
(6) F. A. Cotton, B. A. Frenz, G. Deganello, and A. Shaver, *J. Organomet. Chem.*, **50**, 227 (1973).
(7) "International Tables for X-Ray Crystallography", Vol. IV, Kynoch Press, Birmingham, England, 1974.
(8) D. T. Cromer and D. Liberman, *J. Chem. Phys.*, **53**, 1891 (1970).
(9) The calculations were carried out using the following programs: DATARED, a data reduction program by Frenz; FOURIER, a Fourier summation program (based on Zalkin's FORDAP) by Dellaca and Robinson, modified by Hodgson; FAME, a program for calculating normalized structure factors by Dewar; HYDROGEN, a program for calculating atom positions in certain arrangements by Frenz and Stanislowski; NUCLS, a full-matrix least-squares program by Ibers and Doedens, similar to Busing and Levy's ORFLS; SADIAN, a distances and angles program by Baur, rewritten by Frenz; ORFFE, a function and error program by Busing, Martin, and Levy as modified by Brown, Johnson, and Theissen; ORTEP, a plotting program by Johnson; LIST, a program for listing the data by Snyder.
(10) Supplementary material.
(11) G. H. Stout and L. H. Jensen, "X-Ray Structure Determination", Macmillan, New York, N.Y., 1972.
(12) F. A. Cotton, Z. C. Mester, and T. R. Webb, *Acta Crystallogr., Sect. B*, **30**, 2768 (1974).
(13) F. A. Cotton and J. G. Norman, Jr., *J. Coord. Chem.*, **1**, 161 (1971).
(14) F. A. Cotton, J. G. Norman, Jr., B. R. Stults, and T. R. Webb, *J. Coord. Chem.*, in press.
(15) F. A. Cotton and T. R. Webb, *Inorg. Chem.*, **15**, 68 (1976).
(16) J. G. Norman, Jr., and H. J. Kolari, *J. Chem. Soc., Chem. Commun.*, 649 (1975), and private communications from J. G. Norman, Jr.
(17) F. A. Cotton, T. LaCour, and A. G. Stanislowski, *J. Am. Chem. Soc.*, **96**, 754 (1974); F. A. Cotton and A. G. Stanislowski, *ibid.*, **96**, 5074 (1974).
(18) F. A. Cotton and V. W. Day, *J. Chem. Soc., Chem. Commun.*, 416 (1974).
(19) Recent examples are found in the following references: (a) G. Avitabile, P. Ganis, and M. Nemeroff, *Acta Crystallogr., Sect. B*, **27**, 725 (1971); (b) C. S. Arcus, J. L. Wilkinson, C. Mealli, T. J. Marks, and J. A. Ibers, *J. Am. Chem. Soc.*, **96**, 7564 (1974); (c) R. J. Restivo, G. Ferguson, D. J. O'Sullivan, and F. J. Lalor, *Inorg. Chem.*, **14**, 3046 (1975).
(20) F. A. Cotton and J. G. Norman, Jr., *J. Am. Chem. Soc.*, **94**, 5697 (1972).
(21) F. A. Cotton, *Inorg. Chem.*, **4**, 334 (1965).
(22) J. G. Norman, Jr., and H. J. Kolari, *J. Am. Chem. Soc.*, **97**, 33 (1975).
(23) A. P. Mortola, J. W. Moskowitz, and N. Rosch, *Int. J. Quantum Chem. Symp.*, **No. 8**, 161–167 (1974).

Contribution from the Department of Chemistry, Texas A&M University, College Station, Texas 77843

The Scrambling of Carbonyl Groups in Guaiazulenehexacarbonyldimolybdenum and Two Isomeric Triethylphosphine Substitution Products

F. ALBERT COTTON,* PASCUAL LAHUERTA, and B. RAY STULTS

Received March 8, 1976 AIC601784

Two isomeric compounds with the formula (guaiazulene)$Mo_2(CO)_5(PEt_3)$ have been prepared and identified structurally by means of x-ray crystallography. They differ in the location of the PEt_3 group, which is on a different molybdenum atom in each case. The carbon-13 NMR spectra of both derivatives have been studied from the slow- to the fast-exchange limits. From the entire pattern of chemical shift changes which occur it has been possible to deduce for the parent hexacarbonyl (**1**) that it is the $Mo(CO)_3$ group bonded to the cyclopentadienyl group that executes internal scrambling of its CO groups more rapidly. The structure of the isomer (**2**) with the PEt_3 group attached to the molybdenum atom that is bound to the five-membered ring was refined isotropically to convergence (R_1 = 0.071, R_2 = 0.099). The crystals belong to the monoclinic system, space group $P2_1/a$, with a = 14.379 (11) Å, b = 14.569 (7) Å, c = 13.034 (6) Å, β = 94.67 (5)°. The PEt_3 group is found along the extension of the Mo–Mo bond. The structure of the isomer (**3**) was refined with anisotropic temperature parameters for the two molybdenum atoms and the phosphorus atom and isotropic temperature parameters for all other atoms to final residuals of 0.111 and 0.155. The crystals contain a disordered molecule of CH_2Cl_2 which we have not fully defined, thus accounting for the relatively high R values even though the molecular structure parameters have acceptable accuracy. The crystals belong to the space group $P2_1/c$ with a = 16.151 (10) Å, b = 12.336 (8) Å, c = 15.558 (9) Å, β = 104.27 (6)°, and V = 3004 (4) Å^3.

We have previously reported[1] that in the guaiazulenehexacarbonyldimolybdenum complex, **1**, there is a local scrambling process in each of the $Mo(CO)_3$ groups, but no general or intermetal scrambling up to the temperature range

for decomposition (ca. 85 °C). The feature of particular interest was the marked difference between the activation energies for local scrambling on each of the two $M(CO)_3$ groups. For one, the coalescence temperature was appreciably below −112 °C and for the other the coalescence temperature was about −35 °C. Assuming identical frequency factors of ca. 10^{13} for both $Mo(CO)_3$ groups, the temperature difference of about 100 °C corresponds to a difference in activation energy of about 5 kcal mol^{-1}.

This observation raises two interesting questions: (1) Can we determine, experimentally, which group is fast and which is slow? The experimental results for **1** alone do not provide an answer to this question. (2) Can we understand, in terms of bonding theory, why these two groups, which differ only in that one is bonded to a pentadienyl and the other to a cyclopentadienyl group, should differ so markedly in their rates and activation energies?

We decided to try first to obtain an experimental answer to question 1 and, for the moment at least, to leave question 2 in abeyance. Our method of approach, suggested by an earlier study of (cyclooctatriene)$Fe_2(CO)_6$ and related systems,[2,3] was to replace one CO group by triethylphosphine, identify by x-ray crystallography the isomer obtained, and then observe and interpret the changes caused in the NMR spectra. Fortunately, in this case each of the two possible products, with PEt_3 on each of the Mo atoms, was obtained and characterized, thus allowing an unambiguous answer to question 1. In addition, we were interested in the effects of PEt_3 substitution at one metal atom upon the chemical shifts and tendency to engage in scrambling of the CO groups on the other metal atom, since earlier work had given some unexpected, and unexplained, results of that sort. Thus, the elucidation of the substituent effects in themselves, as well as their use in interpreting the behavior of the parent molecule, was also an objective of this investigation.

Experimental Section

Preparative. (Guaiazulene)$Mo_2(CO)_6$, **1**, was prepared according to the literature.[4] The isomeric substitution products, **2** and **3**, of composition (guaiazulene)$Mo_2(CO)_5PEt_3$, were prepared as follows. Compound **1**, 0.25 g (0.50 mmol), and triethylphosphine, 0.15 ml (1.2 mmol), were refluxed in 60 ml of heptane for 3 h under an atmosphere of N_2. After removal of solvent under reduced pressure, the resulting residue was dissolved in a 1:1 mixture of CH_2Cl_2 and hexane and chromatographed on a Florisil column. When the same solvent mixture was used to develop the chromatogram the following four bands were observed: (1) A fast-moving blue band consisting of guaiazulene. (2) A dark-red band consisting of unreacted **1**. (3) A yellow-brown band, very closely following the second band. The compound forming this band is designated **2**. (4) A very slow-moving red band, which was more efficiently eluted using pure CH_2Cl_2. The compound forming this band is designated **3**. By slowly concentrating the solutions of bands 3 and 4, crystalline samples of compounds **2** and **3** were obtained. The ir spectra of **2** and **3** (CS_2 solutions) in the CO stretching region consisted of the following bands (cm^{-1}). **2**: 1977 (s), 1920 (s), 1890 (s), 1860 (m), 1810 (s). **3**: 1965 (s) 1905 (s), 1895 (s).

NMR Measurements. Carbon-13 spectra were recorded on a Jeol-100/Nicolet 1080 Fourier transform spectrometer at a spectrometer frequency of 25.035 MHz. The ^2H signal of the solvent was used for locking. Samples of **1** were enriched to ca. 20% in ^{13}CO by stirring a solution of the isotopically normal compound in CH_2Cl_2 under a ^{13}CO atmosphere. The enriched **1** was then reacted with PEt_3 in the manner described above to produce enriched **2** and **3**.

The spectra were recorded at various temperatures down to −110 °C using as solvent a mixture of CH_2Cl_2/CD_2Cl_2 in the ratio 70 to 25% and also containing 5% CS_2. The latter served as an internal chemical shift reference. Trisacetylacetonatochromium(III), 5 mg, was added to each sample.

X-Ray Crystallographic Study of Compound 2. X-ray data were collected using a black crystal grown from a CH_2Cl_2 solution into which hexane was allowed to diffuse slowly at 0 °C. This crystal was mounted and sealed in a capillary. The approximate dimensions of the crystal were 0.25 × 0.30 × 0.30 mm.

Preliminary x-ray examination of the crystal and data collection were performed on a Syntex $P\bar{1}$ computer-controlled diffractometer equipped with a graphite-crystal monochromator in the incident beam. The crystal was found to be monoclinic. Systematic absences in the data set subsequently collected ($0k0$ for $k \neq 2n$, $h0l$ for $h \neq 2n$) indicated the space group to be $P2_1/a$. The widths at half-height (ω scans) of several strong reflections were found to be <0.20°. Cell constants were obtained by carefully centering 15 reflections in the range $25° < 2\theta < 30°$; the cell constants and calculated volume are a = 14.379 (11) Å, b = 14.569 (7) Å, c = 13.034 (6) Å, β = 94.67 (5)°, and V = 2721 (3) Å^3. The linear absorption coefficient for Mo Kα radiation is 10.3 cm^{-1}; absorption corrections were therefore omitted.

Intensities were measured at 22 ± 4 °C using the θ–2θ scan method. With Mo Kα radiation, 3507 independent reflections were measured in the 2θ range from 0 to 45°. Scan speeds varied from 4 to 24° min^{-1}, and the scan range was from 0.8° below the Kα_1 peak to 0.8° above the Kα_2 peak. No significant change in the standards was observed. Lorentz and polarization corrections were applied to the data.

The position of one of the Mo atoms was determined from a three-dimensional Patterson map.[5] Two cycles of refinement gave discrepancy indices of $R_1 = \sum||F_o| - |F_c||/\sum|F_o| = 0.59$ and $R_2 = (\sum w(|F_o| - |F_c|)^2/\sum w|F_o|^2)^{1/2} = 0.66$. The second Mo atom was located in a difference Fourier map and refined (R_1 = 0.35, R_2 = 0.44). The P atom, five carbonyl groups, and nine ring carbon atoms were found in a new difference Fourier map and refined (R_1 = 0.20, R_2 = 0.28). All the rest of the atoms were located in a third difference Fourier map and refined isotropically to convergence (R_0 = 0.07I, R_2 = 0.099). In this refinement only those 2903 reflections with $I > 3\sigma(I)$ were used. A value of P = 0.06 was used in the calculation of σ.[5]

Atomic positional parameters and isotropic thermal parameters are listed in Table I. Bond distances and angles are given in Tables II and III.

X-Ray Crystallographic Study of Compound 3. X-ray data were collected using a dark red crystal grown from a solution of the compound in Cl_2CH_2:hexane (1:1) at 0 °C. This crystal was mounted

Table I. Atomic Positional Parameters and Isotropic Thermal Parameters for Compound **2**

Atom	x	y	z	β
Mo1	0.34735 (6)	0.29978 (6)	0.25881 (7)	2.78 (3)
Mo2	0.25372 (6)	0.48962 (6)	0.33584 (7)	2.79 (3)
P	0.3669 (2)	0.1475 (2)	0.1872 (2)	3.19 (6)
O1	0.2266 (7)	0.1920 (6)	0.4046 (7)	5.6 (2)
O2	0.1937 (7)	0.3081 (7)	0.0756 (7)	6.4 (2)
O3	0.1319 (6)	0.3589 (6)	0.4625 (6)	4.9 (2)
O4	0.1259 (6)	0.4858 (6)	0.1285 (7)	5.3 (2)
O5	0.0988 (7)	0.6273 (7)	0.3850 (7)	5.8 (2)
C1	0.4809 (7)	0.3782 (7)	0.2031 (8)	3.3 (2)
C2	0.5116 (8)	0.3016 (7)	0.2640 (8)	3.6 (2)
C3	0.4866 (8)	0.3133 (7)	0.3675 (8)	3.7 (2)
C4	0.3888 (7)	0.4366 (7)	0.4563 (8)	3.3 (2)
C5	0.3685 (8)	0.5278 (7)	0.4703 (8)	3.4 (2)
C6	0.3570 (8)	0.6023 (7)	0.3976 (8)	3.6 (2)
C7	0.3644 (7)	0.5990 (7)	0.2885 (8)	3.3 (2)
C8	0.3813 (7)	0.5198 (7)	0.2317 (8)	3.2 (2)
C9	0.4430 (7)	0.4364 (7)	0.2661 (7)	3.0 (2)
C10	0.4364 (7)	0.3956 (7)	0.3690 (7)	3.0 (2)
C11	0.5027 (9)	0.3959 (9)	0.0928 (9)	4.7 (3)
C12	0.3868 (8)	0.3734 (8)	0.5504 (9)	4.2 (2)
C13	0.3565 (9)	0.6886 (9)	0.2274 (10)	4.5 (3)
C14	0.2797 (12)	0.7529 (12)	0.2671 (13)	7.1 (4)
C15	0.4406 (14)	0.7351 (13)	0.2153 (14)	8.1 (4)
C16	0.2706 (8)	0.2350 (8)	0.3461 (8)	3.6 (2)
C17	0.2521 (8)	0.3079 (8)	0.1454 (9)	4.0 (2)
C18	0.1767 (7)	0.4051 (7)	0.4113 (8)	3.4 (2)
C19	0.1744 (8)	0.4844 (7)	0.2081 (8)	3.5 (2)
C20	0.1594 (8)	0.5772 (8)	0.3698 (9)	4.1 (2)
C21	0.2544 (8)	0.0861 (9)	0.1577 (9)	4.5 (3)
C22	0.4398 (8)	0.0643 (8)	0.2664 (9)	4.1 (2)
C23	0.4261 (8)	0.1401 (8)	0.0668 (9)	4.2 (2)
C24	0.2612 (10)	−0.0091 (10)	0.1072 (11)	6.0 (3)
C25	0.4017 (11)	0.0394 (11)	0.3695 (12)	6.4 (3)
C26	0.3757 (10)	0.1900 (9)	−0.0231 (11)	5.4 (3)

Table II. Bond Distances in Compound **2**[a]

(i) Distances from Molybdenum Atoms (Å)			
Mo1-Mo2	3.270 (2)	Mo1-P	2.433 (3)
Mo1-C1	2.40 (1)	Mo2-C4	2.52 (1)
Mo1-C2	2.36 (1)	Mo2-C5	2.37 (1)
Mo1-C3	2.36 (1)	Mo2-C6	2.31 (1)
Mo1-C9	2.34 (1)	Mo2-C7	2.37 (1)
Mo1-C10	2.31 (1)	Mo2-C8	2.41 (1)
Mo1-C16	1.90 (1)	Mo2-C18	1.97 (1)
Mo1-C17	1.94 (1)	Mo2-C19	1.94 (1)
		Mo2-C20	1.94 (1)
(ii) Distances within the Bicyclic Ring System			
C1-C2	1.42 (2)	C4-C5	1.38 (1)
C2-C3	1.43 (2)	C5-C6	1.44 (1)
C3-C10	1.40 (1)	C6-C7	1.44 (1)
C10-C9	1.46 (1)	C7-C8	1.40 (1)
C9-C1	1.40 (1)	C8-C9	1.48 (1)
		C10-C4	1.50 (1)
(iii) Other Distances within the Guaiazulene Ligand			
C1-C11	1.52 (2)	C7-C13	1.54 (2)
C4-C12	1.54 (2)	C13-C15	1.53 (2)
		C13-C14	1.47 (2)
(iv) Carbon-Oxygen Distances			
C16-O1	1.20 (1)	C19-O4	1.20 (1)
C17-O2	1.19 (1)	C20-O5	1.17 (1)
C18-O3	1.18 (1)		
(v) Distances within the Phosphine Ligand			
P-C21	1.86 (1)	C21-C24	1.54 (2)
P-C22	1.86 (1)	C22-C25	1.53 (2)
P-C23	1.85 (1)	C23-C26	1.51 (2)

[a] Figures in parentheses are the estimated standard deviations in the least significant figures.

Table III. Bond Angles in Compound **2**[a]

(i) Around Molybdenum Atoms (deg)			
Mo2-Mo1-P	162.35 (8)	Mo1-Mo2-C18	83.5 (3)
Mo2-Mo1-C16	87.9 (3)	Mo1-Mo2-C19	86.1 (3)
Mo2-Mo1-C17	84.2 (3)	Mo1-Mo2-C20	160.0 (3)
C16-Mo1-C17	94.5 (5)	C18-Mo2-C19	95.1 (5)
C16-Mo1-P	82.4 (3)	C18-Mo2-C20	82.3 (5)
C17-Mo1-P	81.9 (3)	C19-Mo2-C20	81.3 (5)
(ii) Within Carbonyl Ligands			
Mo1-C16-O1	176.2 (10)	Mo2-C18-O3	175.0 (9)
Mo1-C17-O2	176.6 (10)	Mo2-C19-O4	176.7 (9)
		Mo2-C20-O5	175.5 (11)
(iii) Angles within the Guaiazulene Nucleus			
C2-C1-C9	107.1 (9)	C4-C10-C9	123.4 (9)
C1-C2-C3	110.0 (9)	C8-C9-C10	126.2 (9)
C2-C3-C10	106.5 (9)	C7-C8-C9	128.5 (9)
C3-C10-C9	108.2 (9)	C6-C7-C8	125.4 (10)
C1-C9-C10	108.1 (9)	C5-C6-C7	127.8 (10)
		C4-C5-C6	130.9 (10)
C1-C9-C8	125.5 (9)	C5-C4-C10	126.9 (9)
C3-C10-C4	128.3 (9)		
(iv) Angles for Substituents on the Guaiazulene Ligand			
C2-C1-C11	125.7 (10)	C6-C7-C13	117.5 (9)
C9-C1-C11	127.0 (10)	C8-C7-C13	117.0 (9)
C10-C4-C12	114.0 (9)	C7-C13-C15	108.4 (12)
C5-C4-C12	117.1 (9)	C7-C13-C14	116.5 (11)
		C14-C13-C15	111.3 (13)
(v) Around Phosphorus Atom			
Mo1-P-C21	113.1 (4)	C21-P-C22	104.0 (5)
Mo1-P-C22	117.4 (4)	C21-P-C23	104.4 (5)
Mo1-P-C23	117.0 (4)	C22-P-C23	99.0 (5)
(vi) Angles within the Phosphine Ligand			
P-C21-C24	115.8 (9)	P-C23-C26	113.9 (9)
P-C22-C25	114.5 (9)		

[a] Figures in parentheses are the estimated standard deviations in the least significant figures.

in a sealed glass capillary and had approximate dimensions of 0.20 × 0.25 × 0.30 mm.

Scheme I

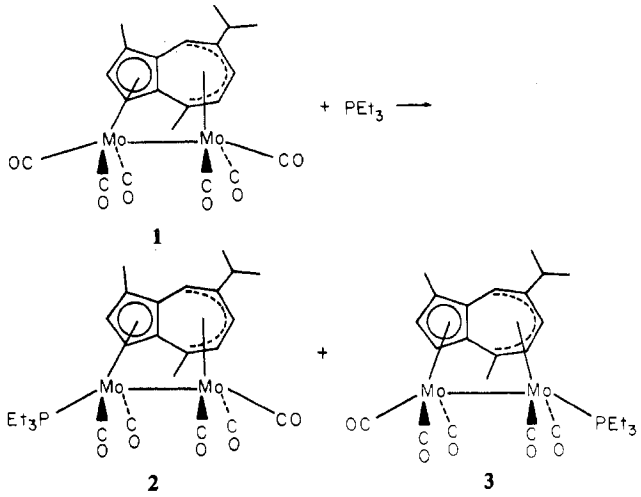

The crystal was monoclinic. Systematic absences in the subsequent data set indicated the space group to be $P2_1/c$. Proceeding as above for compound **2**, the following cell constants and volume were obtained: $a = 16.151$ (10) Å, $b = 12.336$ (8) Å, $c = 15.558$ (9) Å, $\beta = 104.27$ (6)°, and $V = 3004$ (4) Å^3. Intensities were measured as reported for compound **2**. The 3972 independent reflections were collected in the 2θ range from 0 to 45°. No significant change was observed in the standards. As for compound **2**, no absorption correction was applied and the data were reduced to a set of relative $|F_{obsd}|^2$ after Lorentz and polarization corrections.

The position of one Mo atom was determined from a three-dimensional Patterson map. Two cycles of refinement gave $R_1 = 0.57$ and $R_2 = 0.64$. The second Mo atom and the P atom were located from a difference Fourier map and refined giving $R_1 = 0.32$ and $R_2 = 0.41$. A series of three difference Fourier maps (each following least-squares refinement of the atoms located up to that point) resulted in location of the 34 unique atoms of the molecule. The difference in unit cell volumes (3004 (4) Å^3 for **3** and 2721 (3) Å^3 for **2**) suggested that the unit cell of compound **3** contained from two to four solvent molecules, most likely CH_2Cl_2. A difference Fourier map after isotropic refinement of the 34 atoms revealed several peaks about the crystallographic inversion centers at (0, 0, $^1/_2$; 0, $^1/_2$, 0). Several peaks, between 2.5 and 2.7 Å from the inversion centers, were consistent with the presence of a disordered CH_2Cl_2 molecule at each inversion center. Two attempts were made to refine an assumed model for the disordered CH_2Cl_2 molecule with little or no improvement in the R values and no effect upon the structural parameters. Since the primary purpose of this structure determination was to identify compound **3** and reveal, qualitatively, its structure, no further attempts were made to refine a model for the disordered solvent molecule in order to save time and computer costs. In the final cycle of full-matrix least-squares refinement, the two molybdenum atoms and the phosphorus atom were refined with anisotropic thermal parameters to give final residuals $R_1 = 0.111$ and $R_2 = 0.155$.

Atomic positional parameters and the refined thermal parameters are listed in Table IV. Bond distances and bond angles are given in Tables V and VI. A list of the observed and calculated structure factor amplitudes for both compounds is available as indicated in the paragraph at the end of this paper entitled Supplementary Material Available.

Results

As a consequence of the x-ray crystallographic work, the reaction of **1**, (guaiazulene)$Mo_2(CO)_6$, with PEt_3 is now known to produce two products, **2** and **3**, as indicated in Scheme I. Compound **2** forms brown solutions and black crystals. Compound **3** is red both in solution and as a solid.

The solid-state structures of compounds **2** and **3** have been determined with moderate accuracy by x-ray crystallography. Refinement was terminated in both cases at the stage of isotropic convergence, although atoms Mo1, Mo2, and P were refined anisotropically for compound **3**, since the greater

Table IV. Atomic Positional Parameters and Refined Thermal Parameters for Compound **3**[a]

Atom	x	y	z	β_{11}	β_{22}	β_{33}	β_{12}	β_{13}	β_{23}
Mo1	0.1717 (2)	−0.0347 (2)	0.1247 (1)	0.0075 (2)	0.0065 (1)	0.00271 (8)	−0.0003 (3)	0.0007 (2)	−0.0001 (2)
Mo2	0.2622 (2)	0.1192 (2)	0.2932 (1)	0.0070 (2)	0.0053 (1)	0.00296 (8)	−0.0001 (3)	0.0009 (2)	0.0000 (2)
P	0.3455 (6)	0.2775 (5)	0.3604 (4)	0.0085 (5)	0.0060 (5)	0.0047 (3)	−0.0010 (9)	0.0029 (7)	−0.0011 (6)

Atom	x	y	z	B, Å^2	Atom	x	y	z	B, Å^2
O1	0.119 (1)	0.152 (1)	−0.011 (1)	5.9 (4)	C12	0.041 (2)	0.199 (2)	0.198 (2)	5.6 (7)
O2	0.150 (1)	−0.180 (2)	−0.043 (7)	7.9 (5)	C13	0.314 (2)	0.000 (2)	0.510 (2)	4.5 (6)
O3	0.256 (1)	0.265 (2)	0.126 (1)	7.3 (5)	C14	0.265 (2)	−0.057 (3)	0.569 (2)	8.0 (9)
O4	0.442 (1)	0.020 (2)	0.298 (1)	7.9 (5)	C15	0.382 (2)	−0.069 (2)	0.507 (2)	6.8 (7)
O5	0.355 (2)	−0.052 (2)	0.107 (1)	9.2 (6)	C16	0.145 (2)	0.080 (2)	0.040 (2)	4.7 (6)
C1	0.145 (2)	−0.168 (2)	0.229 (1)	4.2 (5)	C17	0.159 (2)	−0.124 (2)	0.019 (2)	6.8 (7)
C2	0.065 (2)	−0.146 (2)	0.161 (2)	5.7 (7)	C18	0.258 (2)	0.201 (2)	0.186 (2)	5.9 (7)
C3	0.036 (2)	−0.036 (2)	0.166 (1)	4.2 (5)	C19	0.372 (2)	0.053 (2)	0.294 (1)	4.4 (5)
C4	0.098 (2)	0.130 (2)	0.265 (1)	4.5 (5)	C20	0.296 (2)	−0.042 (2)	0.113 (2)	7.0 (7)
C5	0.139 (2)	0.173 (2)	0.345 (1)	3.4 (5)	C21	0.293 (2)	0.397 (3)	0.394 (2)	7.1 (8)
C6	0.209 (2)	0.129 (2)	0.417 (2)	4.4 (6)	C22	0.423 (2)	0.242 (2)	0.469 (2)	5.7 (6)
C7	0.252 (2)	0.025 (2)	0.423 (1)	4.1 (5)	C23	0.419 (2)	0.347 (3)	0.293 (2)	8.0 (8)
C8	0.244 (2)	−0.052 (2)	0.353 (1)	4.2 (5)	C24	0.228 (2)	0.448 (3)	0.320 (2)	7.6 (9)
C9	0.166 (2)	−0.068 (2)	0.277 (1)	3.5 (5)	C25	0.483 (2)	0.335 (3)	0.513 (2)	8.5 (9)
C10	0.102 (2)	0.015 (2)	0.238 (2)	5.1 (6)	C26	0.482 (2)	0.271 (3)	0.261 (2)	8.2 (9)
C11	0.193 (2)	−0.269 (2)	0.251 (2)	5.0 (6)					

[a] The form of the anisotropic thermal parameters is: $\exp[-(\beta_{11}h^2 + \beta_{22}k^2 + \beta_{33}l^2 + \beta_{12}hk + \beta_{13}hl + \beta_{23}kl)]$.

Table V. Bond Distances in Compound **3**[a]

(i) Distances from Molybdenum Atoms (Å)

Mo1-Mo2	3.274 (1)	Mo2-P	2.454 (4)
Mo1-C1	2.423 (12)	Mo2-C4	2.581 (15)
Mo1-C2	2.380 (15)	Mo2-C5	2.405 (13)
Mo1-C3	2.436 (15)	Mo2-C6	2.303 (13)
Mo1-C9	2.425 (11)	Mo2-C7	2.372 (12)
Mo1-C10	2.397 (14)	Mo2-C8	2.348 (12)
Mo1-C16	1.907 (13)	Mo2-C18	1.936 (15)
Mo1-C17	1.950 (17)	Mo2-C19	1.949 (17)
Mo1-C20	2.060 (25)		

(ii) Distances within the Bicyclic Ring System

C1-C2	1.48 (2)	C4-C5	1.36 (2)
C2-C3	1.45 (2)	C5-C6	1.49 (2)
C3-C10	1.50 (2)	C6-C7	1.45 (2)
C10-C9	1.47 (2)	C7-C8	1.43 (2)
C9-C1	1.44 (2)	C8-C9	1.52 (2)
		C10-C4	1.49 (2)

(iii) Other Distances within the Guaiazulene Ligand

C1-C11	1.46 (2)	C7-C13	1.50 (2)
C4-C12	1.48 (2)	C13-C14	1.52 (2)
		C13-C15	1.39 (2)

(iv) Carbon-Oxygen Distances

C16-O1	1.20 (1)	C19-O4	1.19 (2)
C17-O2	1.16 (2)	C20-O5	1.00 (2)
C18-O3	1.21 (2)		

(v) Distances within the Phosphine Ligand

P-C21	1.84 (2)	C21-C24	1.51 (2)
P-C22	1.89 (1)	C22-C25	1.54 (2)
P-C23	1.96 (2)	C23-C26	1.56 (2)

[a] Figures in parentheses are in the estimated standard deviations in the least significant figures.

Table VI. Bond Angles in Compound **3**[a]

(i) Angles around the Molybdenum Atoms (deg)

Mo2-Mo1-C16	95.7 (4)	Mo1-Mo2-P	153.2 (1)
Mo2-Mo1-C17	159.7 (5)	Mo1-Mo2-C18	72.6 (4)
Mo2-Mo1-C20	81.1 (5)	Mo1-Mo2-C19	89.5 (4)
C16-Mo1-C17	83.2 (6)	C18-Mo2-P	81.3 (4)
C16-Mo1-C20	91.5 (5)	C18-Mo2-C19	93.6 (6)
C17-Mo1-C20	78.6 (7)	C19-Mo2-P	85.7 (4)

(ii) Within the Carbonyl Groups

Mo1-C16-O1	172 (1)	Mo2-C18-O3	172 (1)
Mo1-C17-O2	178 (2)	Mo2-C19-O4	175 (1)
Mo1-C20-O5	175 (2)		

(iii) Angles within the Azulene Nucleus

C2-C1-C9	105 (1)	C4-C10-C9	129 (1)
C1-C2-C3	112 (1)	C8-C9-C10	126 (1)
C2-C3-C10	104 (1)	C7-C8-C9	126 (1)
C3-C10-C9	109 (1)	C6-C7-C8	126 (1)
C1-C9-C10	110 (1)	C5-C6-C7	129 (1)
C1-C9-C8	124 (1)	C4-C5-C6	131 (1)
C3-C10-C4	123 (1)	C5-C4-C10	125 (1)

(iv) Angles for Substituents on the Azulene Ligand

C2-C1-C11	129 (1)	C6-C7-C13	117 (1)
C9-C1-C11	125 (1)	C8-C7-C13	117 (1)
C10-C4-C12	114 (1)	C7-C13-C15	108 (1)
C5-C4-C12	120 (1)	C7-C13-C14	117 (1)
		C14-C13-C15	106 (1)

(v) Angles around the Phosphorus Atom

Mo2-P-C21	121.2 (6)	C21-P-C22	100.3 (7)
Mo2-P-C22	111.8 (5)	C21-P-C23	100.4 (8)
Mo2-P-C23	117.4 (5)	C22-P-C23	102.9 (7)

(vi) Angles within the Phosphorus Ligand

P-C21-C24	114 (1)	P-C23-C26	116 (1)
P-C22-C25	115 (1)		

[a] Figures in parentheses are the estimated standard deviations in the least significant figures.

accuracy which complete anisotropic refinement might afford would serve no useful purpose in this study. Since the observed structure factor amplitudes are available in the microfilm edition, additional refinement could be carried out by anyone to whom this might be of interest. The structures and atom labeling schemes for compounds **2** and **3** are shown in Figures 1 and 2, respectively. Corresponding atoms within the guaiazulene rings have identical labels to facilitate comparisons. Within the combined experimental uncertainties of the three structural determinations (see ref 6 for the structure of **1**), there are no differences between the common portions of compounds **1**, **2**, and **3**. The Mo–Mo distances are 3.267 (1), 3.270 (2), and 3.274 (1) Å for **1**, **2**, and **3**, respectively. The Mo–P distances are 2.433 (3) Å for **2** and 2.454 (4) Å for **3**.

Table VII. ^{13}CO NMR Spectra of Compounds **1**, **2**, and **3**

Compd	Temp, °C	Signals[a] ($^2J_{P-C}$, Hz)		
1	−112	32.8	29.6	26.3
	+28	32.6	27.4	
2	22	42.2 (17.65)	37.4 (20.59)	32.2
3	22	39.8 (17.67)	36.3 (19.27)	34.4

[a] Chemical shifts are downfield from internal CS_2.

The carbon-13 NMR spectra in the carbonyl region for compounds **2** and **3** are shown in Figure 3 and the numerical

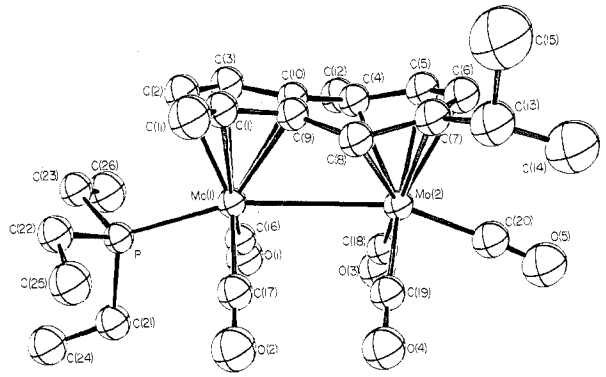

Figure 1. The molecular structure of compound **2**. Atoms are represented by spheres with radii proportional to their isotropic thermal vibration parameters. The atom numbering scheme used in the tables is defined.

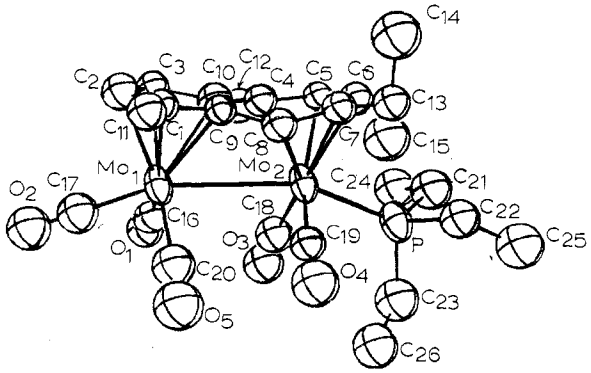

Figure 2. The molecular structure of compound **3**. Atoms are represented by spheres with radii proportional to their thermal vibration parameters. The atom numbering scheme used in the tables is defined.

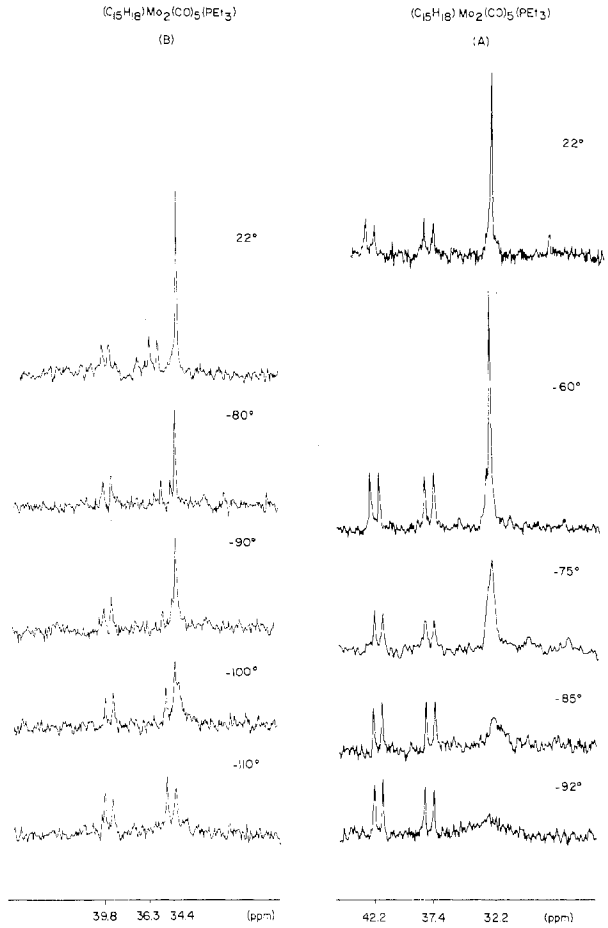

Figure 3. Carbon-13 NMR spectra of the isomeric (guaiazulene)-$Mo_2(CO)_5PEt_3$ molecules. Isomer A (right) is compound **2**; isomer B (left) is compound **3**.

values of the chemical shifts and spin–spin splittings are recorded in Table VII.

Discussion

The work described here had two objectives. The first was to determine which $Mo(CO)_3$ group in the parent molecule, **1**, is the more internally labile and the second was to learn more about the effects of phosphine substitution at one metal atom upon the behavior of the CO groups attached to the other in an $(OC)_nM-M'(CO)_m$ species.

In order to determine which NMR signals arise from each of the $Mo(CO)_3$ groups of **1**, we employ arguments based upon the changes in chemical shifts for each of the isomers obtained when the Et_3P ligand replaces a CO ligand. In order to employ such arguments it is helpful to have independent results from other systems which show what magnitudes may be expected for the shifts of CO groups that are on the substituted metal atom and for the CO groups on the adjacent, unsubstituted metal atom. Fortunately, the results of several such independent studies are available.

For the $[(\eta^5\text{-}C_5H_5)Mo(CO)_3]_2$ (**4**) and $(\eta^5\text{-}C_5H_5)Mo(CO)_3\text{–}Mo(CO)_2(PPh_3)(\eta^5\text{-}C_5H_5)$ (**5**) pair we have the following results.[7] In **4** there are two equivalent CO groups each trans to the Mo–Mo bond and four CO groups that are all cis to the Mo–Mo bond. Signals for these occur respectively at 43.0 and 34.2 ppm downfield from CS_2. The spectrum of **5** shows conclusively that PPh_3 occupies one trans site. Thus on the substituted Mo atom there are two, equivalent CO ligands which give rise to a doublet (J_{P-C} = 50 Hz) at 43.1 ppm; the shift caused by the substitution of PPh_3 for CO on the same metal atom is thus 8.9 ppm. The cis carbonyl groups on the unsubstituted metal atom give a signal at 36.8 ppm, so that the shift is 2.6 ppm. The trans CO on the unsubstituted metal atom gives a signal at 44.6 ppm, meaning that the shift caused by substitution on the adjacent metal atom is 1.6 ppm. In summary, the substitution of one CO group by the phosphine, PPh_3, causes the positions of all ^{13}CO signals to move downfield but for the CO groups on the substituted metal atom the shift is large (8.9 ppm) while for those on the other metal atom the shifts (1.6 and 2.6 ppm) are much smaller.

Similarly, we have previously reported[3] on $(C_{10}H_{12})Fe_2(CO)_6$ and $(C_{10}H_{12})Fe_2(CO)_5PEt_3$. Again, all ^{13}CO resonances are shifted downfield. For those on the substituted metal atom the average shift is 5.0 ppm, while the average shift for those on the other atom is 3.0 ppm.

A downfield shift of all remaining CO resonances is also to be expected on theoretical grounds, since the high shielding of carbon nuclei in MCO groups is due in large part to the M → C dative π bonding.[8] Replacement of any one CO ligand by a phosphine must lead to increased M → C dative π bonding at all of the remaining ones. It is also reasonable to expect that those CO groups on the metal atom which bears the PR_3 substituent will experience a greater effect than those on the adjacent metal atom. Thus theory and experimental data are in unison and lead to the following generalization, which is applicable to compounds **1**, **2**, and **3**: (1) All ^{13}CO signals must move downfield. (2) The signals for CO groups on the substituted metal atom must shift more than those for the CO groups on the adjacent metal atom.

We now compare the chemical shifts in **1** with those in **2** and **3**, using in each case the two possibilities for assigning the spectrum of **1**. In each case we use the positions of the

Table VIII. Downfield Shifts of ^{13}CO Resonances for **2** and **3** from **1** for the Two Possible Assignments of **1**

Assignment for **1**	 $-Mo(CO)_3$			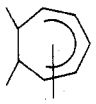 $-Mo(CO)_3$		
	δ_i	$\delta_2-\delta_1$	$\delta_3-\delta_1$	δ_i	$\delta_2-\delta_1$	$\delta_3-\delta_1$
A	32.6			27.4		
	40.0	7.4		32.2	4.8	
	34.4		1.8	38.1		11.7
B	27.4			32.6		
	40.0	12.6		32.2	−0.4	
	34.4		7.0	38.1		5.5

singlets observed in the fast-exchange limits. These comparisons are set out in Table VIII. The two possible assignments, A and B, are defined as follows. A: the "fast" $Mo(CO)_3$ group, 32.6 ppm, is assigned to the cyclopentadienyl ring B: the "slow" $Mo(CO)_3$ group, 27.4 ppm, is assigned to the cyclopentadienyl ring.

It is evident that only the results for assignment A are in agreement with the two empirical rules. For assignment B the rules are violated for both **2** and **3**. For **2**, one of the shifts is slightly upfield (−0.4) instead of downfield. For **3**, the relative magnitudes of the shifts for the two sets of CO groups are the inverse of what they should be, i.e., greater for those on the *un*substituted atom.

Since assignment A is correct, we conclude that it is the $Mo(CO)_3$ group bonded to the cyclopentadienyl ring which has the lower activation energy for internal CO scrambling in the parent molecule, **1**.

In our earlier study[3] of $C_{10}H_{12}Fe_2(CO)_5PEt_3$ we observed that when a CO group on one $Fe(CO)_3$ unit was replaced by PEt_3, the coalescence temperature for scrambling of the CO groups on the other $Fe(CO)_3$ moiety was substantially lowered, namely by about 45 °C. We did not know whether an effect of this sort would be general. The results for compounds **1**, **2**, and **3** presented here leave this point still somewhat ambiguous. A comparison of compounds **1** and **2** reveals the same effect observed with the iron compound; the coalescence temperature for the $Mo(CO)_3$ group attached to the seven-membered ring drops from about −35 to about −95 °C, an even greater drop than the one observed earlier. On the other hand, for compound **3** the coalescence temperature for the $Mo(CO)_3$ group attached to the five-membered ring appears to be around −110 °C, which is not lower, and possibly a little higher than the corresponding one in compound **1**. The nature of these neighboring substituent effects thus remains puzzling and not even empirically predictable.

Another effect observed here (see Figure 3 and Table VII) is the large chemical shift difference between the two CO groups remaining on the substituted Mo atom. These differences are 4.8 and 3.5 ppm in compounds **2** and **3**, respectively. We find this surprising and do not have a ready explanation for it.

Acknowledgment. We thank Dr. Douglas L. Hunter for his contributions to the earlier phases of this study and Dr. Douglas M. Collins for some discussions concerning the crystallography. Financial support was provided in part by the National Science Foundation (Grant No. 33142X) and by the Commission on Cultural Exchange between Spain and the United States of America through a fellowship to P.L.

Registry No. **1**, 59414-35-6; **2**, 59350-36-6; **3**, 59350-35-5; triethylphosphine, 554-70-1; ^{13}C, 14762-74-4.

Supplementary Material Available: Tables of the observed and calculated structure factor amplitudes for compounds **2** and **3** (29 pages). Ordering information is given on any current masthead page.

References and Notes

(1) F. A. Cotton, D. L. Hunter, and P. Lahuerta, *J. Organomet. Chem.*, **87**, C42 (1975).
(2) F. A. Cotton, D. L. Hunter, and P. Lahuerta, *J. Am. Chem. Soc.*, **97**, 1046 (1975).
(3) F. A. Cotton and D. L. Hunter, *J. Am. Chem. Soc.*, **97**, 5739 (1975).
(4) R. Burton, L. Pratt, and G. Wilkinson, *J. Chem. Soc.*, 4290 (1960).
(5) Programs for data reduction as well as those used subsequently in the structure analysis are as follows: DATARED by Frenz was used for data reduction. AGNOST, used for the absorption correction, is a modification by Frenz of Cohen's AGNOST. The Fourier program JIMDAP by Ibers is a version of Zalkin's FORDAP. NUCLS, a full-matrix least-squares program by Ibers and Doedens, closely resembles Busing and Levy's ORFLS program; the function minimized in the refinement is $\sum w(|F_o| - |F_c|)^2$. ORTEP by Johnson was used for drawing illustrations on a Gerber plotter. Atomic distances, angles, and errors were calculated using program ORFFE by Busing, Martin, and Levy as modified by Brown, Johnson, and Thiessen. Final structural refinement of compound **3** was conducted using a PDP 11/45 computer and the Enraf Nonius SDP computer programs at the Molecular Structure Corporation, College Station, Texas.
(6) M. R. Churchill and P. H. Bird, *Inorg. Chem.*, 7, 1545 (1968).
(7) These data are from unpublished studies in this laboratory by Dr. John R. Kolb.
(8) H. Mahnke, R. K. Sheline, and H. W. Spiess, *J. Chem. Phys.*, **61**, 55 (1974).

Contribution No. 5256 from the A. A. Noyes Laboratory, California Institute of Technology, Pasadena, California 91125

Distinguishing between Inner- and Outer-Sphere Electrode Reactions. Reactivity Patterns for Some Chromium(III)–Chromium(II) Electron-Transfer Reactions at Mercury Electrodes

MICHAEL J. WEAVER and FRED C. ANSON*

Received January 16, 1976 AIC60046A

Two methods for distinguishing between inner- and outer-sphere electrode reaction mechanisms for a certain class of metal complexes are described and applied to several complexes of Cr(III). One method is based on the response of the reaction rate to the addition of strongly adsorbed but chemically inactive anions. The second method depends upon differences in the potential dependence of the reaction rate for inner- and outer-sphere pathways. Electrochemical reactivity differences spanning eight orders of magnitude were measured for a series of eight complexes of Cr(III) of the type $Cr(OH_2)_5X$. The origin of the large range of reactivities is discussed in terms of "intrinsic" and "thermodynamic driving force" differences. It is suggested that the latter factor is dominant with outer-sphere reactants whereas both factors can contribute significantly to the relative reactivities of inner-sphere reactants.

Introduction

Efforts directed toward the identification of the electrode reaction mechanisms of simple, one-electron redox reactions of transition metal ion complexes have been both less extensive and less successful than is true for the analogous homogeneous redox reactions. A primary factor contributing to the greater